



Fermi National Accelerator Laboratory

FERMILAB-Conf-99/164-E

CDF

CDF Run II Discovery Reach for Neutral MSSM Higgs Bosons via
 $p\bar{p} \rightarrow b\bar{b}\varphi \rightarrow b\bar{b}b\bar{b}$

J.A. Valls

For the CDF Collaboration

Rutgers, The State University of New Jersey

*Fermi National Accelerator Laboratory
P.O. Box 500, Batavia, Illinois 60510*

July 1999

Presented at *Physics at Run II: Workshop on Supersymmetry/Higgs: Summary Meeting*,
Fermilab, Batavia, Illinois, November 19-21, 1998

Disclaimer

This report was prepared as an account of work sponsored by an agency of the United States Government. Neither the United States Government nor any agency thereof, nor any of their employees, makes any warranty, expressed or implied, or assumes any legal liability or responsibility for the accuracy, completeness, or usefulness of any information, apparatus, product, or process disclosed, or represents that its use would not infringe privately owned rights. Reference herein to any specific commercial product, process, or service by trade name, trademark, manufacturer, or otherwise, does not necessarily constitute or imply its endorsement, recommendation, or favoring by the United States Government or any agency thereof. The views and opinions of authors expressed herein do not necessarily state or reflect those of the United States Government or any agency thereof.

Distribution

Approved for public release; further dissemination unlimited.

Copyright Notification

This manuscript has been authored by Universities Research Association, Inc. under contract No. DE-AC02-76CHO3000 with the U.S. Department of Energy. The United States Government and the publisher, by accepting the article for publication, acknowledges that the United States Government retains a nonexclusive, paid-up, irrevocable, worldwide license to publish or reproduce the published form of this manuscript, or allow others to do so, for United States Government Purposes.

CDF Run II Discovery Reach for Neutral MSSM Higgs Bosons via $p\bar{p} \rightarrow b\bar{b}\varphi \rightarrow b\bar{b}b\bar{b}$

Juan A. Valls

Rutgers, The State University of New Jersey

Abstract. In this paper we examine the CDF Run II discovery reach for neutral Higgs bosons via the process $p\bar{p} \rightarrow b\bar{b}\varphi \rightarrow b\bar{b}b\bar{b}$. The signature is a four jet final state with at least three b -tagged jets. Signal and background acceptances are estimated using the CDF Run I detector performance. b tagging efficiencies and fake tag rates are evaluated with new Run II increased detector geometrical acceptances. Total rates are estimated from present Run I data and from Monte Carlo. The results are interpreted within the framework of the minimal supersymmetric extension of the standard model (MSSM) and generalized in terms of a model independent enhancement factor.

INTRODUCTION

One of the most important goals of present and future high energy colliders is to reveal the mechanism responsible for electroweak symmetry breaking. In the standard model (SM) of electroweak interactions the Higgs mechanism introduces spontaneous symmetry breaking by the introduction of a scalar field doublet. This leaves a single observable scalar particle, the Higgs boson, with unknown mass but fixed couplings to other particles. The minimal supersymmetric extension of the standard model (MSSM) is the best motivated extension of the SM where some of their theoretical problems are solved. After electroweak symmetry breaking the Higgs sector of the MSSM requires a spectrum of five elementary Higgs particles: two neutral CP-even scalars, h and H , one CP-odd pseudoscalar, A , and two charged Higgs bosons, H^\pm . In order to describe the MSSM Higgs sector, one has to introduce four masses, M_h , M_H , M_A , and M_{H^\pm} and two additional parameters, which describe the properties of the scalar particles and their interactions with gauge bosons and fermions: the mixing angle β , related to the ratio of the two vacuum expectation values, $\tan\beta = v_2/v_1$, and the mixing angle α in the neutral CP-even sector.

The MSSM predictions for the Higgs boson masses are of important phenomenological consequences. The lightest CP-even Higgs boson mass M_h is constrained to $M_h \lesssim 130$ GeV [1] while the masses of the other Higgs bosons are expected to be larger and, in some cases, degenerate.

Associated Production $p\bar{p} \rightarrow b\bar{b}\varphi \rightarrow b\bar{b}b\bar{b}$

In this paper, we search for $p\bar{p} \rightarrow b\bar{b}\varphi \rightarrow b\bar{b}b\bar{b}$ events at $\sqrt{s} = 1.8$ TeV. Two typical Feynman diagrams for these processes at lowest order are shown in Figure 1. Although this process is produced in the SM with limited rates ($\lesssim 10^{-2}$ pb), it is particularly favored in some models where the b quark Yukawa coupling is enhanced relative to the standard model prediction. In particular, in the MSSM scenario the $b\bar{b}A$ coupling is proportional to $\tan\beta$ and thus, the cross section grows with $\tan^2\beta$ with respect to the standard model. In addition, the $b\bar{b}$ decay mode dominates the neutral Higgs decay modes for large $\tan\beta$. For small $\tan\beta$ the $b\bar{b}$ decay modes are still dominant for $M_\varphi \leq 150$ GeV/ c^2 . In the large $\tan\beta$ region, one of the CP-even scalar Higgs is degenerate with the pseudoscalar A , and its couplings to $b\bar{b}$ pairs has essentially the same strength as the $b\bar{b}A$ coupling. For small M_A values this degenerate state is the light CP-even scalar Higgs boson h , while for larger M_A it is the heavy CP-even scalar Higgs boson H .

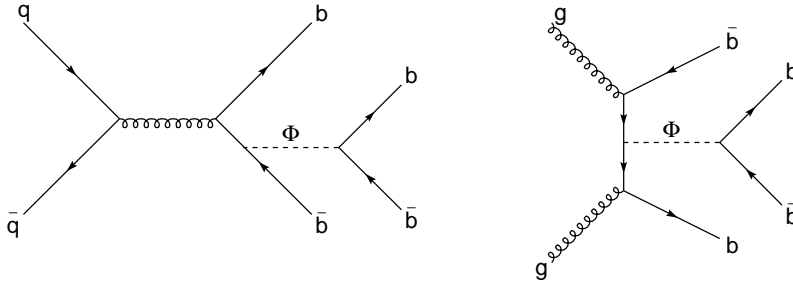


FIGURE 1. Typical lowest order Feynman diagrams contributing to the process $p\bar{p} \rightarrow b\bar{b}\varphi \rightarrow b\bar{b}b\bar{b}$.

Figure 2 show the expected rates for $b\bar{b}\varphi \rightarrow b\bar{b}b\bar{b}$ production at large $\tan\beta$ as a function of the Higgs mass. In this regime ($\tan\beta \gtrsim 20$) φ is either h or A for masses below the light Higgs upper bound, or either the H or A for masses above the light Higgs upper limit. All rates are shown for the case of vanishing mixing parameters or non-mixing case defined by $\mu = A_t = A_b = 0$ with μ the Higgs mass parameter and A_t and A_b the soft SUSY Yukawa breaking parameters. In all cases, a top quark mass of $M_t = 175 \text{ GeV}/c^2$ and a SUSY mass scale of $M_S = 1 \text{ TeV}$ are assumed. To calculate the Yukawa coupling we use a running bottom quark mass evaluated at the Higgs mass scale ($M_b \simeq 3 \text{ GeV}/c^2$). All cross sections are evaluated at leading order (LO) with the CTEQ3 parton distributions functions and the renormalization scale equal to the Higgs mass.

Signal Monte Carlo Simulation

For signal modelling we used a modified version of the parton level Monte Carlo program PAPAGENO [2] together with the Lund PYTHIA v5.6 string fragmentation and hadronization program [3]. Fixed weight $p\bar{p} \rightarrow b\bar{b}\varphi$ events with $\varphi \rightarrow b\bar{b}$ are generated at leading order (LO) and fragmented inside PYTHIA. The mass of the Higgs has been set to values between $M_\varphi = 70 \text{ GeV}/c^2$ to $300 \text{ GeV}/c^2$. In order to setup parton showers and fragmentation inside PYTHIA, the color-flow information for colored particles is treated properly. Both initial and final state showering are allowed at energy scales corresponding to the Higgs mass. After fragmentation, events are then passed through the CDF Run I simulation and reconstruction code.

EVENT SELECTION

The CDF Run I multijet trigger requirements are used as the first step in the data selection. This sample is defined by events that satisfy:

- a) total trigger cluster $\sum E_T^{L2} > 125 \text{ GeV}$, and
- b) 4 trigger clusters with $E_T^{L2} > 15 \text{ GeV}$

where a level 2 (L2) trigger cluster is defined by a nearest-neighbor reconstruction algorithm, seeded by a tower of $E_T > 3 \text{ GeV}$ and including only towers of $E_T > 1 \text{ GeV}$. The event selection follows by requiring events with at least four offline reconstructed jets with $E_T > 15 \text{ GeV}$ and $|\eta| \leq 2.1$. Jets are defined as localized energy depositions in the calorimeters and are reconstructed using an iterative clustering algorithm with a fixed cone of radius $\Delta R = \sqrt{\Delta\eta^2 + \Delta\phi^2} = 0.4$ in $\eta - \phi$ space. Jet energies are then corrected for energy losses in uninstrumented detector regions, energy falling outside the clustering cone, contributions from underlying event and multiple interactions, and calorimeter nonlinearities.

The typical topology of the signal events consist of two primary b quarks and a Higgs φ , which is radiated from one of the primary b quarks. There is, thus, a very high energetic primary b quark with momentum of the order of the mass of the Higgs boson, M_φ , balanced by the Higgs and the other primary b quark, which is generally much softer. The Higgs decays into a $b\bar{b}$ pair with typical transverse momentum of the order of $M_\varphi/2$. The four highest- E_T (uncorrected) jets in the event are then ordered in E_T :

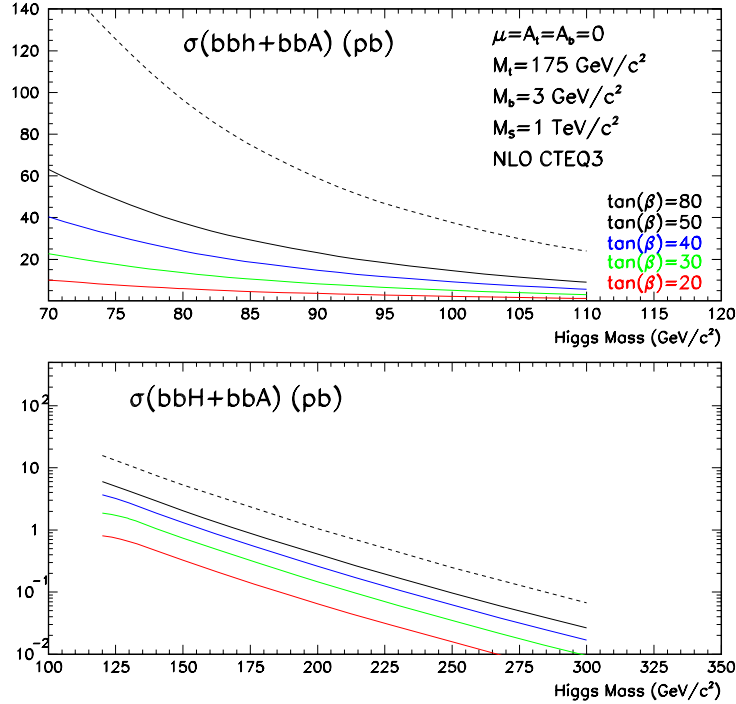


FIGURE 2. Production cross sections for $(b\bar{b}h + b\bar{b}A) \rightarrow b\bar{b}b\bar{b}$ (upper plot) and $(b\bar{b}H + b\bar{b}A) \rightarrow b\bar{b}b\bar{b}$ (lower plot) as a function of the Higgs mass. The two plots correspond to the different degenerate states, $M_h = M_A$ for Higgs masses below the light Higgs upper bound, and $M_H = M_A$ for Higgs masses above the light Higgs upper bound. Results are shown for $\tan\beta \geq 20$ and the non-mixing scenario.

TABLE 1. Optimized E_T thresholds for the three highest E_T jets in the event as a function of the signal mass.

	M (GeV/ c^2)											
	70	80	90	100	110	120	130	140	150	200	250	300
E_{T1} (GeV)	40	40	42	42	46	48	50	54	58	75	95	120
E_{T2} (GeV)	32	32	32	34	34	34	38	38	42	55	72	85
E_{T3} (GeV)	14	14	14	14	14	14	14	14	14	40	55	70

$$E_T^1 \geq E_T^2 \geq E_T^3 \geq E_T^4 \quad (1)$$

and a mass dependent requirement made for E_T^1 , E_T^2 , and E_T^3 . The E_T thresholds for these cuts are shown in Table 1 as a function of the Higgs mass. They have been optimized by maximizing the significance of the signal. Figure 3 shows the the E_T^j , $j = 1, 2, 3, 4$ distributions for two different signal Higgs masses ($M = 120, 250$ GeV/ c^2) compared with the QCD background shapes.

We then require that at least three among the four highest- E_T jets in the event are identified (tagged) as b quark candidates. We use the CDF secondary vertex algorithm [4] with the intrinsic Run I efficiencies and mistag rates per jet inside the SVX fiducial region. The results are then applied to b jets at generator level within the increased geometrical acceptance of the Run II CDF silicon vertex detector (SVX II). The SVX II extends the b -tagging capabilities up to the range $|\eta| < 2$. The b -tagging algorithm begins by searching for secondary vertices that contain three or more displaced tracks. If none are found, the algorithm searches for two-track vertices using more stringent track criteria. A jet is tagged if the secondary vertex transverse displacement from the primary one exceeds three times its uncertainty.

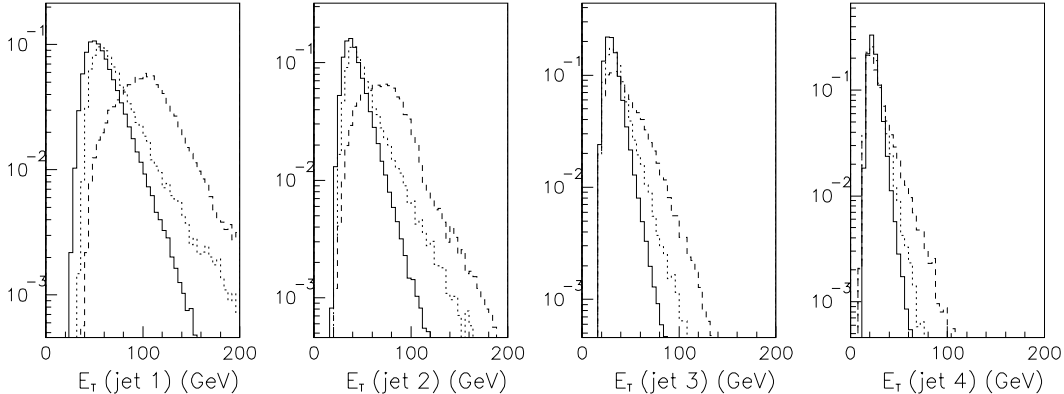


FIGURE 3. Transverse energy distributions for the four leading jets in the event. The solid histograms correspond to QCD background. The dashed and dotted histograms correspond to signal masses of $M = 250$ and $120 \text{ GeV}/c^2$ respectively.

Table 2 shows the trigger efficiency (ϵ_{trig}), E_T^j efficiencies ($\epsilon_{E_T^j}$), double b -tag ($\epsilon_{\geq 2b}$) and triple b -tag ($\epsilon_{\geq 3b}$) efficiencies, and total efficiencies (ϵ_{tot}) as a function of the Higgs mass. The double and triple b -tag efficiencies are calculated after the trigger and E_T^j cuts are applied. The total efficiency applies to the triple b -tag selection. All errors shown are statistical only.

Figure 4 shows the reconstructed dijet invariant mass distribution for different signal masses. The invariant mass of the dijet system is defined as $M_{ij} = \sqrt{2E_T^i E_T^j [\cosh(\Delta\eta)_{ij} - \cos(\Delta\phi)_{ij}]}$. The distributions contain a Gaussian core with a resolution of 10-20% depending slightly on the Higgs mass. To maximize the signal dijet mass resolutions we use the reconstructed invariant mass of the highest- E_T jets in the event for masses $M \geq 120 \text{ GeV}/c^2$. For masses $M < 120 \text{ GeV}/c^2$ we use the invariant mass of the second and third highest- E_T jets in the event. In all cases, the two highest- E_T jets in the event are always required to be tagged. The tails of the distributions are dominated by the cases where the jet assignment in the mass reconstruction is incorrect. In most of these cases, one of the jets assigned to the Higgs is a primary b quark jet.

BACKGROUNDS

Backgrounds for the process $p\bar{p} \rightarrow b\bar{b}\varphi \rightarrow b\bar{b}b\bar{b}$ include all sources of standard model heavy flavor multijet events. These include QCD heavy flavor production, fake multitags, $t\bar{t}$ ($t \rightarrow Wb$, $W \rightarrow q\bar{q}'$), Z + jets ($Z \rightarrow b\bar{b}/c\bar{c}$), $Wb\bar{b}/c\bar{c}$ and $Zb\bar{b}/c\bar{c}$.

QCD

The dominant source of background is QCD heavy flavor production. This is also the main difficult to estimate due to uncertainties in the predicted total rates as well as heavy flavor jet rates. Rather than attempting to estimate the QCD background rates directly from Monte Carlo, instead we follow the approach used in [5] in the search for standard model Higgs bosons via $VH \rightarrow jjb\bar{b}$ ($V = W, Z$). In [5], the CDF Run I multijet data sample was used to calculate first the double b tagged dijet invariant mass distribution. The shape of this distribution is then fit, using a binned maximum-likelihood method, to a combination of signal, QCD heavy flavors, fake double tags and other standard model backgrounds. The QCD heavy flavor and signal

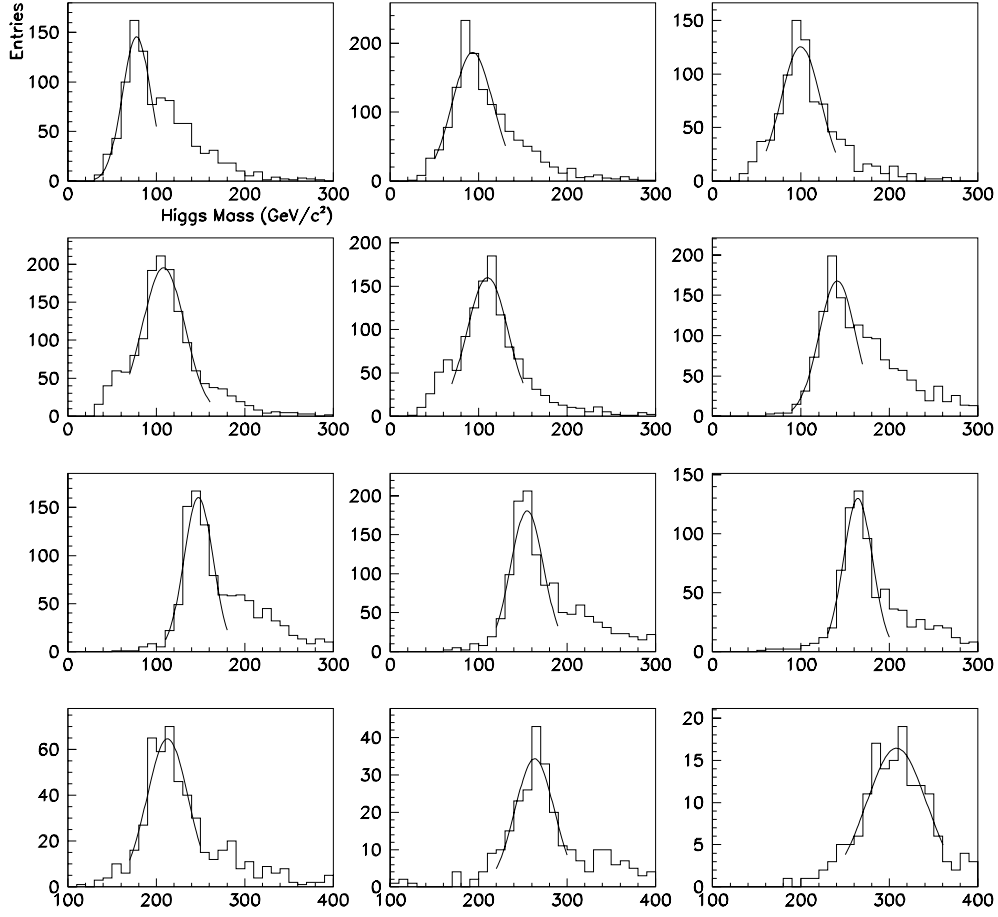


FIGURE 4. Signal dijet invariant mass distributions. From top left the distributions correspond to Higgs masses of $M = 70, 80, 90, 100, 110, 120, 130, 140, 150, 200, 250$ and $300 \text{ GeV}/c^2$, respectively.

TABLE 2. Signal acceptances as a function of the Higgs mass.

M (GeV/c^2)	ϵ_{trig} (%)	$\epsilon_{E_T^j}$ (%)	$\epsilon_{\geq 2b}$ (%)	$\epsilon_{\geq 3b}$ (%)	ϵ_{tot} (%)
70	1.25 ± 0.02	92.7 ± 0.3	78.9 ± 0.7	28.6 ± 0.7	0.33 ± 0.01
80	1.48 ± 0.02	93.0 ± 0.2	78.2 ± 0.6	27.7 ± 0.6	0.38 ± 0.01
90	1.70 ± 0.02	89.7 ± 0.3	79.0 ± 0.8	27.6 ± 0.8	0.42 ± 0.01
100	1.90 ± 0.03	85.8 ± 0.3	78.8 ± 0.6	27.2 ± 0.6	0.44 ± 0.01
110	2.23 ± 0.03	80.7 ± 0.3	76.6 ± 0.6	25.5 ± 0.6	0.46 ± 0.01
120	2.42 ± 0.04	79.6 ± 0.3	77.1 ± 0.8	27.0 ± 0.7	0.52 ± 0.01
130	2.65 ± 0.04	72.8 ± 0.3	77.5 ± 0.7	26.3 ± 0.6	0.51 ± 0.02
140	2.75 ± 0.04	69.5 ± 0.3	77.1 ± 0.8	28.1 ± 0.8	0.54 ± 0.01
150	3.15 ± 0.05	61.6 ± 0.3	79.4 ± 1.0	27.3 ± 1.1	0.53 ± 0.02
200	4.35 ± 0.07	31.3 ± 0.3	82.6 ± 1.3	31.0 ± 1.3	0.42 ± 0.02
250	4.95 ± 0.07	18.5 ± 0.3	78.7 ± 1.5	25.9 ± 1.5	0.24 ± 0.01
300	6.71 ± 0.10	11.5 ± 0.2	79.0 ± 1.5	23.3 ± 1.5	0.18 ± 0.01

TABLE 3. Observed and expected double b -tag events in 91 pb^{-1} of CDF Run I data as obtained from the fit.

	data	QCD heavy flavors	Fakes	$t\bar{t}$	$Z + \text{jets}$
events	589	470 ± 27	85 ± 11	23 ± 6	16 ± 4

TABLE 4. Expected QCD heavy flavor, QCD fake triple tags and total QCD events in 1 fb^{-1} total integrated luminosity.

M (GeV/ c^2)	QCD heavy flavors	QCD fakes	Total QCD
	(events per fb^{-1})		
70	58.6 ± 12.3	12.1 ± 10.5	70.7 ± 16.2
80	58.6 ± 12.3	12.1 ± 10.5	70.7 ± 16.2
90	56.0 ± 11.9	12.1 ± 10.5	68.1 ± 15.9
100	50.6 ± 11.0	12.1 ± 10.5	62.7 ± 15.2
110	48.0 ± 11.0	9.7 ± 7.8	57.7 ± 13.5
120	48.0 ± 11.0	7.3 ± 5.5	55.3 ± 12.3
130	45.3 ± 11.1	7.3 ± 5.5	52.6 ± 12.4
140	29.3 ± 8.0	4.8 ± 3.4	34.1 ± 8.7
150	24.0 ± 7.0	2.4 ± 1.8	26.4 ± 7.2
200	8.0 ± 3.3	1.3 ± 0.8	9.3 ± 3.4
250	0.0 ± 0.0	1.3 ± 0.8	1.3 ± 0.8
300	0.0 ± 0.0	1.3 ± 0.8	1.3 ± 0.8

normalizations are left free in the fit while the rest of backgrounds are constrained by Gaussian functions to their expected values and uncertainties. Fake double tags are estimated from data while the other physics backgrounds are calculated from Monte Carlo. The double b -tag data selection as well as details of the fit can be found in [5]. The fit yields zero signal contribution for the $b\bar{b}\varphi \rightarrow b\bar{b}b\bar{b}$ process for all signal masses. The results of the fit are shown in Table 3. The QCD heavy flavor background expectations are now corrected for the E_T^j ($j = 1, 2, 3$) and triple b -tag acceptances corresponding to the present analysis. QCD heavy flavor acceptances have been calculated with the PYTHIA Monte Carlo program with its QCD leading order $2 \rightarrow 2$ hard scattering processes and parton shower modelling. A sufficiently large number of events were generated with a hard scattering $p_T > 40 \text{ GeV}/c$ in order to obtain unbiased and statistically significant samples. Below this p_T bin no events satisfy the trigger requirements. Fake triple b tag rates are calculated directly from Run I data using fake tagging rate parametrizations. Table 4 shows the expected QCD heavy flavor and QCD fake rates as obtained from data for the selection described in this analysis and after extrapolated to a Run II total integrated luminosity of 1 fb^{-1} .

As a comparison, Table 5 shows the expected initial rates for the individual and total QCD processes leading to heavy flavors in the final state as obtained from PYTHIA. Also shown are the QCD acceptances and expected events for 1 fb^{-1} integrated luminosity for the present analysis. The heavy flavor content in QCD events are conventionally classified in three groups: direct production ($q\bar{q}, gg \rightarrow Q\bar{Q}$), flavor excitation ($Qg \rightarrow Qg$), and gluon splitting ($g \rightarrow Q\bar{Q}$) in initial or final state shower evolution. The relative contributions to the total cross sections are very uncertain and depend on the center of mass energy, the modelling of initial and final state radiation, shower evolution and fragmentation.

TABLE 5. Individual and total cross sections and acceptances for the different QCD hard scattering dijet subprocesses modelled with PYTHIA. Events are generated with a hard scattering $p_T > 40$ GeV/c. The E_T thresholds used to calculate ϵ_{E_T} correspond to the selection for $M = 100$ GeV/c². Last column shows the expected rates for 1 fb⁻¹.

	σ (pb)	ϵ_{trig} (%)	ϵ_{E_T} (%)	$\epsilon_{\geq 2b}$ (%)	$\epsilon_{\geq 3b}$ (%)	ϵ_{tot} (%)	N (events/fb ⁻¹)
	($p_T > 40$ GeV/c)						
$q\bar{q}, gg \rightarrow q\bar{q}$	1.2×10^4	1.23 ± 0.01	63.9 ± 0.3	0.15 ± 0.04	0.0 ± 0.0	0.0 ± 0.0	0.0 ± 0.0
$qq, gg \rightarrow qq, gg$	4.9×10^5	0.98 ± 0.01	60.6 ± 0.3	0.45 ± 0.07	0.04 ± 0.02	0.0002 ± 0.0001	972.6 ± 561.5
$gq \rightarrow gq$	4.4×10^5	1.01 ± 0.01	62.6 ± 0.3	0.45 ± 0.07	0.02 ± 0.02	0.0001 ± 0.0001	593.3 ± 419.5
$gb(c) \rightarrow gb(c)$	3.1×10^4	0.76 ± 0.01	60.3 ± 0.3	3.89 ± 0.20	0.14 ± 0.04	0.0006 ± 0.0002	198.3 ± 57.3
$q\bar{q}, gg \rightarrow b\bar{b}/c\bar{c}$	8.2×10^3	0.94 ± 0.01	62.7 ± 0.2	7.91 ± 0.21	0.19 ± 0.04	0.0011 ± 0.0004	91.9 ± 17.7
Total	9.8×10^5	0.99 ± 0.01	61.6 ± 0.6	0.59 ± 0.05	0.03 ± 0.01	0.0002 ± 0.0001	1856.2 ± 703.5

TABLE 6. Cross sections and acceptances for the $t\bar{t}$ and different W/Z + jets backgrounds. The E_T thresholds correspond to the selection $M = 100$ GeV/c².

	$\sigma \times BR$ (pb)	ϵ_{trig} (%)	ϵ_{E_T} (%)	$\epsilon_{\geq 2b}$ (%)	$\epsilon_{\geq 3b}$ (%)	ϵ_{tot} (%)
$t\bar{t}$	3.49 ± 0.83	92.0 ± 0.8	91.0 ± 0.2	12.3 ± 0.2	0.17 ± 0.03	0.14 ± 0.02
($t \rightarrow Wb \rightarrow jjb$)						
Z +jets	11.8 ± 1.4	30.7 ± 1.2	69.8 ± 0.5	7.5 ± 0.6	0.27 ± 0.10	0.06 ± 0.02
($Z \rightarrow b\bar{b}/c\bar{c}$)						
$Wb\bar{b}/c\bar{c}$	237.2 ± 13.6	28.5 ± 1.1	69.8 ± 0.5	0.06 ± 0.03	0.004 ± 0.003	0.001 ± 0.001
($W \rightarrow q\bar{q}', c\bar{s}$)						
$Zb\bar{b}/c\bar{c}$	74.6 ± 6.4	30.5 ± 1.2	69.8 ± 0.5	0.07 ± 0.03	0.004 ± 0.003	0.001 ± 0.001
($Z \rightarrow q\bar{q}$)						

$$t\bar{t} \rightarrow WbW\bar{b} \rightarrow b\bar{b} + \text{jets}$$

$t\bar{t}$ events have been simulated using the HERWIG [6] v5.6 Monte Carlo generator with $M_t = 175$ GeV/c². The trigger efficiency has been estimated to be $92.0 \pm 0.8\%$ from simulation. The measured CDF cross section of $7.6_{-1.5}^{+1.8}$ [7] is used to estimate the expected number of events. Total $t\bar{t}$ initial rates and acceptances are summarized in Table 6. The errors shown include both statistical and systematic uncertainties. Systematics are dominated by the effect of the absolute energy scale, modelling of initial state radiation in HERWIG, and b -tag efficiencies.

W/Z + jets

The $W/Z + \geq n$ jets background has been studied with a combination of data and Monte Carlo. The CDF measured cross sections for W + jets, $W \rightarrow e\nu$ [8] and Z + jets, $Z \rightarrow ee$ [9] are used to normalize Monte Carlo production cross sections for $W/Z + \geq n$ jet events. Generic W + jets and Z + jets samples generated with the HERWIG Monte Carlo program [10] and processed through the CDF simulation package were used to estimate the expected contributions after our selection cuts. The predominant source of heavy flavor production in $W/Z + \geq n$ jets events is $Z + \geq n$ jets ($Z \rightarrow b\bar{b}/c\bar{c}$) as well as some contribution of initial and final state gluon splitting and higher order diagrams leading to $Wb\bar{b}/c\bar{c}$ and $Zb\bar{b}/c\bar{c}$ events. Table 6 shows the initial cross sections and estimated acceptances for all the W/Z + jets backgrounds leading to heavy flavor final states. The errors shown include both statistical and systematic uncertainties. The systematic uncertainties are dominated by the normalization of the measured cross sections to the predicted Monte Carlo cross sections.

Figure 5 shows the individual and total efficiencies as a function of the Higgs mass for the signal and the different standard model background contributions.

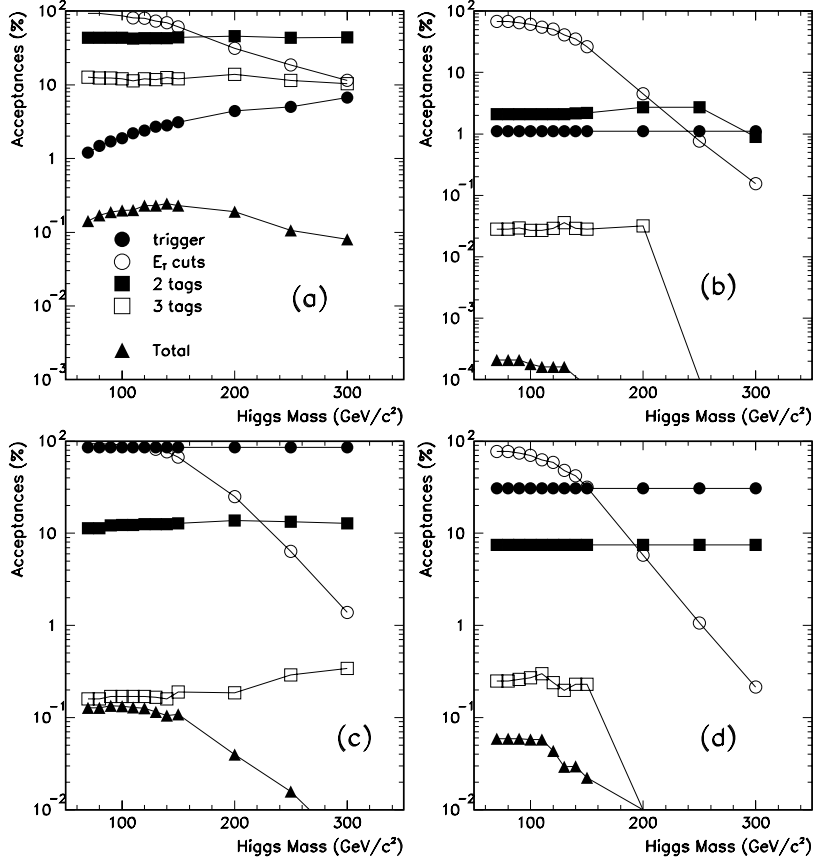


FIGURE 5. Individual and total efficiencies (in %) as a function of the signal mass for (a) signal, (b) QCD, (c) $t\bar{t}$, and (d) $Z + \text{jets}$ ($Z \rightarrow b\bar{b}/c\bar{c}$).

RESULTS

Table 7 shows the expected number of events from each individual background contribution as well as the total backgrounds for 1 fb^{-1} . Table 8 shows the expected number of signal events for $\tan\beta = 10$ (standard model case) and for $\tan\beta = 40$ as well as the signal significances as a function of the Higgs mass for 1 fb^{-1} .

The reconstructed dijet invariant mass for the highest- E_T jets in the event (with both jets required to be b -tagged) and with present CDF Run I dijet resolutions is shown in Figure 6 for both signal and background. All rates are normalized to 1 fb^{-1} .

Figure 7 shows the 95% CL exclusion limits, 3σ discovery thresholds and 5σ discovery thresholds in the $\tan\beta$ vs M_φ plane of the MSSM for four different total integrated luminosity scenarios, $\mathcal{L} = 91 \text{ pb}^{-1}$, 2 fb^{-1} , 10 fb^{-1} and 30 fb^{-1} .

Figure 8 shows the required luminosity for 95% CL exclusion limits, 3σ and 5σ discovery thresholds as a function of the Higgs mass for the MSSM scenario with $\tan\beta = 10$ and 40.

Finally, Figure 9 shows the enhancement factor \mathcal{R} defined as:

$$\sigma_{b\bar{b}b\bar{b}} = \left(\frac{y_b}{y_b^{SM}} \right)^2 \frac{BR(\varphi \rightarrow b\bar{b})}{BR(H^{SM} \rightarrow b\bar{b})} \sigma_{b\bar{b}b\bar{b}}^{SM} = \mathcal{R}^2 \sigma_{b\bar{b}b\bar{b}}^{SM}$$

$$\mathcal{R} = \left(\frac{y_b}{y_b^{SM}} \right) \left[\frac{BR(\varphi \rightarrow b\bar{b})}{BR(H^{SM} \rightarrow b\bar{b})} \right]^{1/2}$$

TABLE 7. Expected number of background events as a function of the Higgs mass for 1 fb^{-1} .

M (GeV/ c^2)	N_{QCD}	N_{Zjj}	$N_{t\bar{t}}$ (events per fb^{-1})	$N_{Wb\bar{b}/c\bar{c}}$	$N_{Zb\bar{b}/c\bar{c}}$	$N_{tot} = B$
70	70.7 ± 16.2	4.4 ± 1.6	13.2 ± 3.5	1.5 ± 0.6	0.5 ± 0.2	90.4 ± 16.7
80	70.7 ± 16.2	4.4 ± 1.6	13.5 ± 3.4	1.5 ± 0.6	0.5 ± 0.2	90.7 ± 16.6
90	68.1 ± 15.9	4.6 ± 1.6	13.4 ± 3.4	1.5 ± 0.6	0.5 ± 0.2	88.1 ± 16.3
100	62.7 ± 15.2	4.5 ± 1.5	13.2 ± 3.2	1.4 ± 0.5	0.5 ± 0.2	82.3 ± 15.6
110	57.7 ± 13.5	4.1 ± 1.5	12.8 ± 3.4	1.3 ± 0.5	0.4 ± 0.2	76.3 ± 14.0
120	55.3 ± 12.3	3.4 ± 1.3	12.6 ± 3.4	1.2 ± 0.5	0.4 ± 0.2	72.9 ± 12.8
130	52.6 ± 12.4	2.1 ± 1.1	12.2 ± 3.2	1.0 ± 0.4	0.3 ± 0.1	68.2 ± 12.9
140	34.1 ± 8.7	1.7 ± 0.6	11.3 ± 3.1	0.8 ± 0.3	0.3 ± 0.1	48.2 ± 9.3
150	26.4 ± 7.2	1.3 ± 0.5	10.8 ± 2.9	0.6 ± 0.2	0.2 ± 0.1	39.3 ± 7.8
200	9.3 ± 3.4	0.0 ± 0.0	4.4 ± 1.2	0.0 ± 0.0	0.0 ± 0.0	13.7 ± 3.6
250	1.3 ± 0.8	0.0 ± 0.0	0.9 ± 0.3	0.0 ± 0.0	0.0 ± 0.0	2.2 ± 0.9
300	1.3 ± 0.8	0.0 ± 0.0	0.3 ± 0.1	0.0 ± 0.0	0.0 ± 0.0	1.6 ± 0.8

TABLE 8. Expected number of SM signal events ($\tan\beta = 1$), MSSM signal events for $\tan\beta = 40$ and significances as a function of the Higgs mass for 1 fb^{-1} .

M (GeV/ c^2)	S ($\tan\beta = 1$)	S/\sqrt{B} ($\tan\beta = 1$)	S ($\tan\beta = 40$)	S/\sqrt{B} ($\tan\beta = 40$)
70	0.039	0.0041	133.2	14.0
80	0.027	0.0028	91.9	9.7
90	0.018	0.0019	62.4	6.6
100	0.012	0.0013	41.0	4.5
110	0.007	0.0008	26.3	3.0
120	0.005	0.0006	19.1	2.2
130	0.002	0.0002	13.7	1.7
140	0.001	0.0001	10.0	1.4
150	0.0004	0.00006	7.0	1.1
200	0.0	0.0	1.1	0.3
250	0.0	0.0	0.15	0.1
300	0.0	0.0	0.03	0.02

also as a function of the Higgs mass, the integrated total luminosity, and for 95% CL, 3σ and 5σ discovery thresholds. The \mathcal{R} factor contains the entire model dependence of the cross section and allows to present the results in a complete model independent way.

CONCLUSIONS

In this paper we have studied the Tevatron Run II sensitivity reach to the neutral MSSM Higgs sector via $b\bar{b}\varphi$ and $\varphi \rightarrow b\bar{b}$. The signature for such process is a four jet final state with at least three b -tagged jets. The data selection is based on a multijet trigger criteria used by CDF in Run I. This trigger was optimized for the all-hadronic top search and is rather inefficient for Higgs searches. Nevertheless, the requirement of displaced tracks with large impact parameter at the trigger level in Run II will make it possible to relax the Run I multijet criteria to only 3 jets with uneven E_T cuts and a lower $\sum E_T$ threshold. A preliminar study [11] shows that these cuts result on a few-fold increase in Higgs signal efficiencies without compromise the total trigger rates. For signal and background modelling we have used the present CDF Run I detector simulation and reconstruction code modified to include b -tagging at the large rapidities covered by the new Run II detectors. Background rates have been estimated from present CDF Run I data and extrapolated to different luminosity scenarios. The results show a sensitivity to a large region in the $\tan\beta$ vs Higgs mass plane of the MSSM with moderate luminosities.

REFERENCES

1. M. Carena, M. Quirós, C.E.M. Wagner, Nucl. Phys. **B461** (1996) 407; H. Haber, R. Hempfling, A. H. Hoang, Z. Phys. **C57** (1997) 539.
2. I. Hinchliffe, Argonne Accel. Phys. **679** (1993).
S. Mrenna and T. Tait, private communication.
3. T. Sjöstrand, Comput. Phys. Commun. **82**, 74 (1994).
4. F. Abe *et al.*, Phys. Rev. Lett. **74**, 2626 (1995).
5. F. Abe *et al.*, Phys. Rev. Lett. **81**, 5748 (1998).
6. G. Marchesini *et al.*, Comput. Phys. Commun. **67**, 465 (1992).
7. F. Abe *et al.*, Phys. Rev. Lett. **80**, 2773 (1998).
8. D. Cronnin-Hennesy *et al.*, *Measurement of $Z \rightarrow ee + N$ jet cross sections in 1.8 TeV $p\bar{p}$ collisions*, CDFnote 3360.
9. D. Cronnin-Hennesy *et al.*, *Measurement of $W^\pm \rightarrow e^\pm\nu + N$ jet cross sections in 1.8 TeV $p\bar{p}$ collisions*, CDFnote 4093.
10. P. Azzi *et al.*, *Evaluation of the $W/Z + jets$ background for the top search in the all-hadronic channel*, CDFnote 3428.
11. P. Maksimovic, Talk at the SUSY/Higgs Workshop, Nov. 6, 1998.

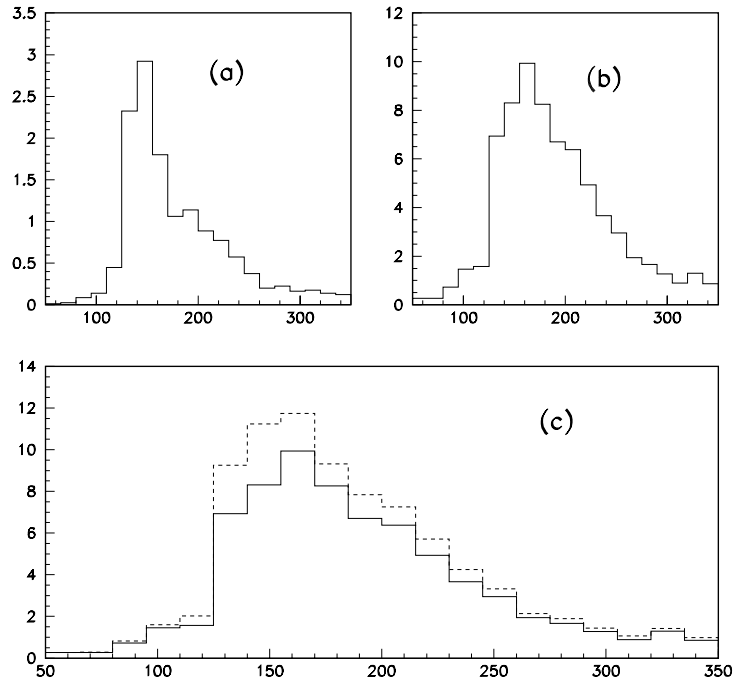


FIGURE 6. Reconstructed dijet invariant mass for the highest- E_T jets in the event for (a) signal ($M = 130 \text{ GeV}/c^2$ and $\tan\beta = 40$), (b) background (QCD, $Z + \text{jets}$ with $Z \rightarrow b\bar{b}/c\bar{c}$ and $t\bar{t}$), and (c) background only (solid histogram) and signal + background (dashed histogram). All distributions are normalized to 1 fb^{-1} of total integrated luminosity.

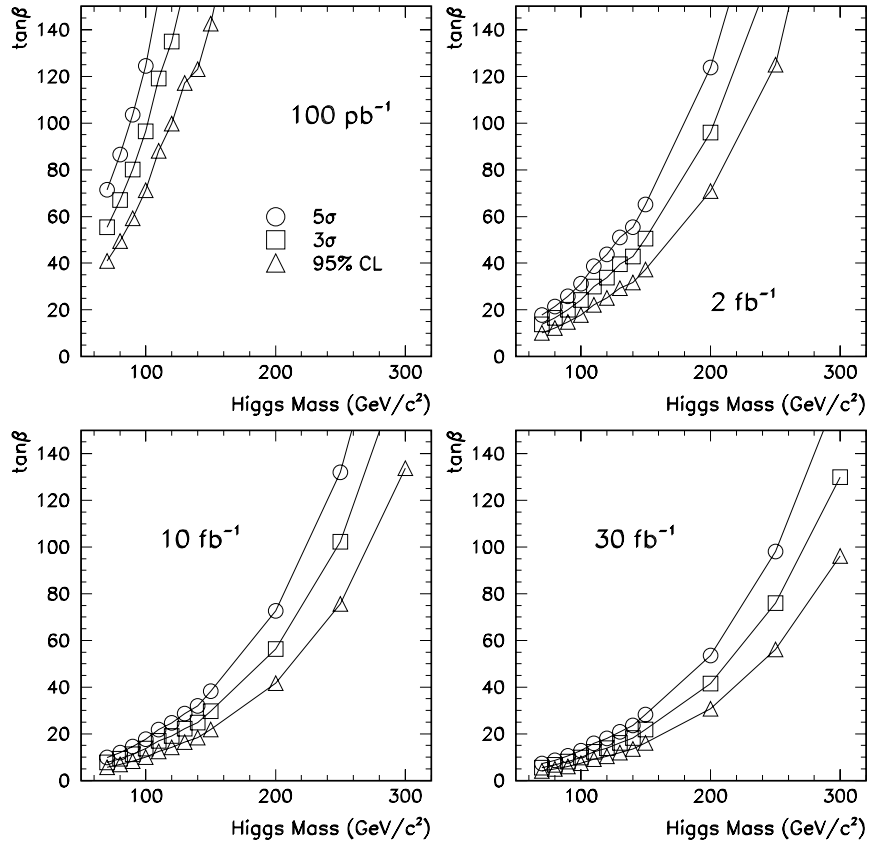


FIGURE 7. Discovery and exclusion contours in the $\tan\beta$ vs M_ϕ plane of the MSSM for total integrated luminosities of 91 pb^{-1} , 2 fb^{-1} , 10 fb^{-1} and 30 fb^{-1} .

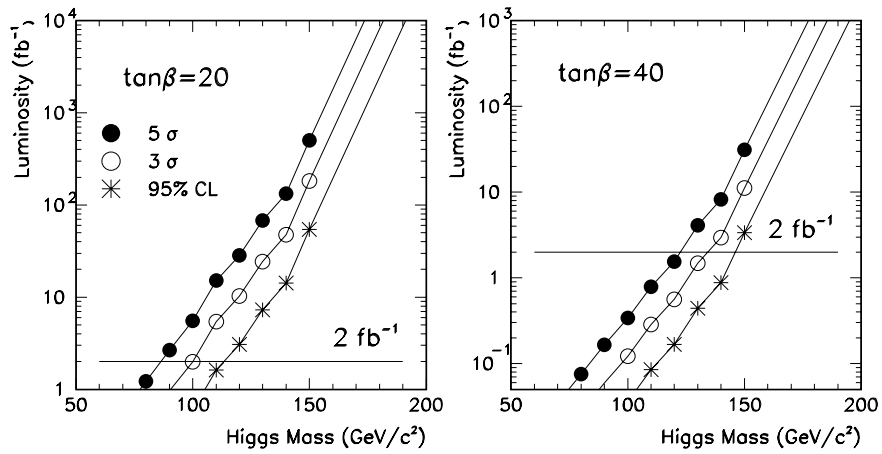


FIGURE 8. Necessary luminosity for 95% CL exclusion limits and 5σ and 3σ discovery thresholds as a function of the Higgs mass for the MSSM scenario with $\tan\beta = 10$ and 40 .

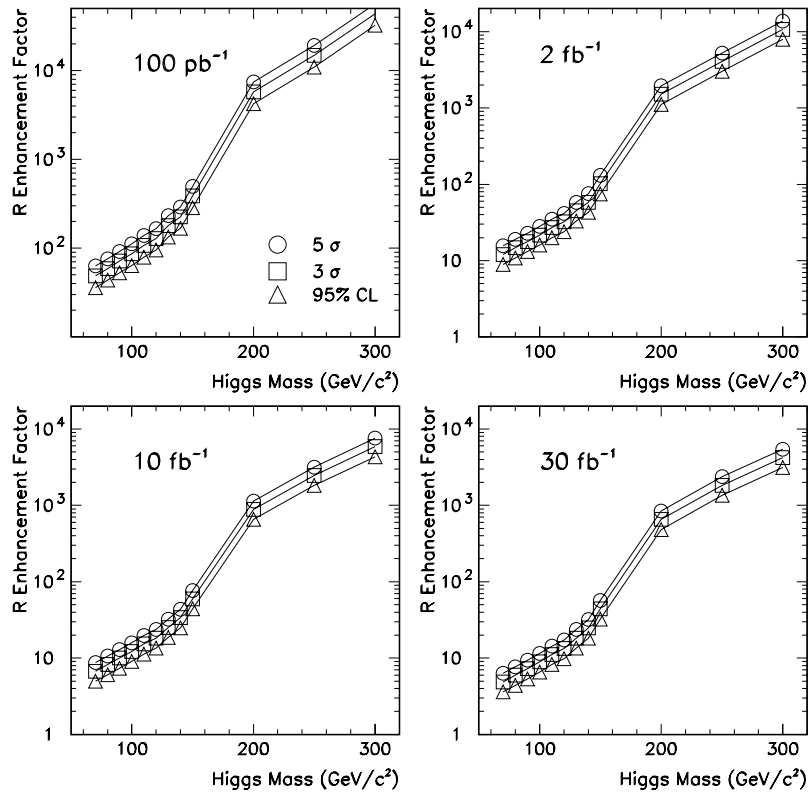


FIGURE 9. Enhancement factor \mathcal{R} as a function of the Higgs mass for 95% CL exclusion limits, 5σ and 3σ discovery thresholds and different total integrated luminosities.